Journal of Cluster Science, Vol. 15, No. 3, September 2004 (© 2004)

Bonding Analysis of Square-Antiprismatic and Fused Square-Antiprismatic Copper(I)-Selenium Clusters

Bachir Zouchoune,[1,2,3] Jean-François Halet,[2] and Jean-Yves Saillard[2]

Received January 13, 2004

The electronic structure of the $Cu_{2(4n+2)}Se_{4n+2}(PH_3)_8$ (n = 1–4) D_{4h} series of model clusters has been analyzed by means of density functional theory calculations. The fused square antiprismatic structure of the metal framework is found to be always preferred over the fused cuboctahedral one because it reinforces the Cu-P bonds. Thus, the presence of the terminal phosphine ligands tends to strengthen the Cu…Cu (d^{10}… d^{10}) bonding by mixing bonding combinations of the vacant Cu 4s and 4p orbitals into the occupied 3d combinations. The calculations indicate that the compounds corresponding to n = 3 and 4 should be easily two-electron-reduced, leading to stable dianionic species.

KEY WORDS: Density functional theory; copper(I)-selenium clusters; d^{10}… d^{10} bonding.

INTRODUCTION

Contrarily to the octahedron [1] or the cube [2], the square antiprism (SA) is not a very common building block in fused polyhedral transition-metal clusters. The few known examples are encountered in the extremely rich chemistry of copper-chalcogen clusters developed by Fenske and collaborators [3], as exemplified by $Cu_{12}Se_6(PEtPh_2)_8$ and $Cu_{20}Se_{10}(PPh_3)_8$ [4] (see **1** and **2** in Fig. 1). Related sulfur species also exist [3, 4]. The former

[1] Laboratoire de Chimie Appliquée et Technologie des Matériaux, Centre Universitaire Larbi Ben M'Hidi, 04000 Oum-El-Bouaghi, and Laboratoire de Chimie Moléculaire, du Contrôle de l'Environnement et des Mesures Physico-Chimiques, Université Mentouri de Constantine, 25000 Constantine, Algérie.

[2] Laboratoire de Chimie du Solide et Inorganique Moléculaire, UMR CNRS 6511, Institut de Chimie, Université de Rennes 1, 35042 Rennes Cedex, France.

[3] To whom correspondence should be addressed.

1040-7278/04/0900-0267/0 © 2004 Plenum Publishing Corporation

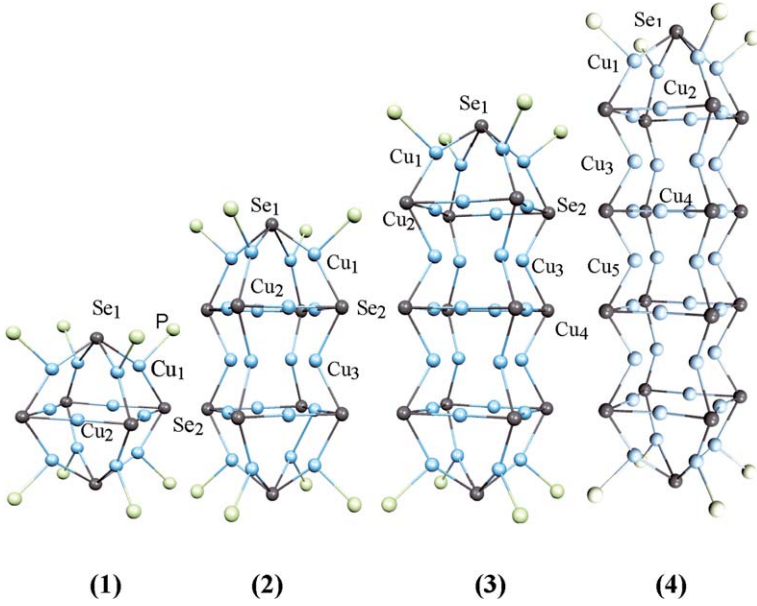

Fig. 1. Molecular structures of the computed models $Cu_{12}Se_6(PH_3)_8$ (**1**), $Cu_{20}Se_{10}(PH_3)_8$ (**2**), $Cu_{28}Se_{14}(PH_3)_8$ (**3**) and $Cu_{36}Se_{18}(PH_3)_8$ (**4**). The experimental structures of $Cu_{12}Se_6(PEtPh_2)_8$ and $Cu_{20}Se_{10}(PPh_3)_8$ [3] are similar to those of **1** and **2**.

exhibits a Cu_{12} skeleton made of two square antiprisms fused through one of their square faces, whereas the Cu_{20} core of the latter is made of four fused square antiprisms. The reported Cu…Cu separations (2.572–2.961 Å) are consistent with the existence of weak Cu(I)…Cu(I) bonding. This type of $d^{10}…d^{10}$ bonding has been described as resulting from the mixing of bonding combinations of the vacant Cu 4s and 4p atomic orbitals into the occupied 3d combinations [5]. Electron correlation has also been shown to be involved in this type of closed shell/closed shell interaction [6]. The copper atoms of the outer copper square faces bear a terminal phosphine ligand. In these compounds of general formula $Cu_{2(4n+2)}Se_{4n+2}(PR_3)_8$ ($n = 1, 2$), the square and rhombohedral faces of the Cu_{2n} polyhedron are capped by μ_4-E atoms in such a way that each Cu atom is bonded to two E atoms. The corresponding E–Cu–E angles are rather open (142°–147°) so that, neglecting the Cu…Cu interactions, the inner Cu atoms can be approximated to 2-coordinated, moderately bent metal centers and the outer Cu atoms can be approximated to planar 3-coordinated metal centers. Theoretical investigations on bare $Cu_{2n}E_n$ species, as well as on $Cu_{12}E_6(PR_3)_8$ (E = S, Se) have been published by

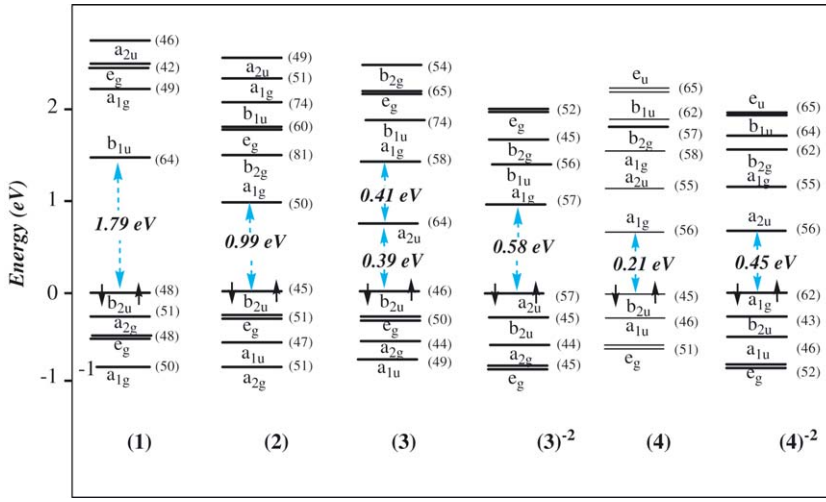

Fig. 2. MO level ordering computed for the neutral compounds **1, 2, 3** and **4** and for the anions $\mathbf{3}^{2-}$ and $\mathbf{4}^{2-}$ (D_{4h} symmetry). The total copper participation (%) is given in parenthesis for each MO.

Ahlrichs and coworkers [4, 7, 8]. In this paper, we focus on larger members built with copper SAs as building blocks and we provide an orbital analysis of their geometry and electronic structure. The following model compounds have been calculated: $Cu_{2(4n+2)}Se_{4n+2}(PH_3)_8$ (n = 1–4). In the following they are labelled as **1**–**4**, respectively. Their molecular structures are shown in Fig. 1 and their MO diagrams are given in Fig. 2. The major computed data are gathered in Table I.

COMPUTATIONAL DETAILS

Density functional theory calculations were carried out using the Amsterdam Density Functional (ADF) package developed by Baerends and coworkers [9]. The results discussed in this paper were obtained assuming the local density approximation of electron correlation using the Vosko–Wilk–Nusair parametrization [10] and nonlocal density approximation assuming corrections of Becke [11] and Perdew [12] for the exchange and correlation energies, respectively. The standard ADF basis set IV was used for the atoms constituting the $Cu_{2n}Se_n$ and $Cu_{2n}Se_n(PH_3)_8$ cores, which describes the valence 3d (Cu), 4s (Cu), 4s (Se), 4p (Se), 3s (P) and 3p (P) and 1s (H) orbitals with triple-ζ Slater-type orbitals. The frozen-core approximation was used to treat the core electrons.

Table I. Selected Computed Data for the Optimized $Cu_{2(4n+2)}Se_{4n+2}(PH_3)_8$ (n = 1–4) D_{4h} Models

Cmpound	$Cu_{12}Se_6(O_h)$	1	$Cu_{20}Se_{10}$	2	3	3^2	4	4^{2-}
Distances (Å) and Cu…Cu Mulliken overlap populations (in parentheses)								
Cu_1–Cu_1	2.658 (0.067)	2.944 (0.025)	2.604 (0.066)	2.872 (0.026)	2.882 (0.024)	2.862 (0.027)	2.924 (0.024)	2.903 (0.027)
Cu_1–Cu_2	2.658 (0.067)	2.732 (0.054)	2.714 (0.066)	2.743 (0.060)	2.783 (0.059)	2.763 (0.059)	2.711 (0.060)	2.721 (0.060)
Cu_2–Cu_2	3.759 (0.001)	3.196 (0.004)	3.404 (0.005)	3.172 (0.017)	3.022 (0.017)	2.995 (0.025)	3.242 (0.017)	2.974 (0.021)
Cu_2–Cu_3	–	–	2.786 (0.061)	2.854 (0.041)	2.744 (0.040)	2.775 (0.039)	2.704 (0.041)	2.716 (0.036)
Cu_3–Cu_3	–	–	2.720 (0.046)	3.221 (0.028)	3.033 (0.026)	2.968 (0.048)	3.021 (0.027)	2.867 (0.046)
Cu_3–Cu_4	–	–	–	–	2.728 (0.045)	2.728 (0.044)	2.701 (0.043)	2.709 (0.041)
Cu_4–Cu_4	–	–	–	–	2.972 (0.016)	2.922 (0.028)	2.952 (0.014)	2.954 (0.022)
Cu_4–Cu_5	–	–	–	–	–	–	2.752 (0.040)	2.712 (0.043)
Cu_5–Cu_5	–	–	–	–	–	–	2.955 (0.001)	2.863 (0.011)
Cu_2–Se_2	2.453	2.383	2.413	2.380	2.313	2.320	2.375	2.396
Cu_1–Se_1	2.453	2.460	2.443	2.524	2.386	2.396	2.463	2.494
Cu_2–Se_2	2.453	2.383	2.425	2.465	2.448	2.453	2.391	2.413
Cu_1–P	–	2.431	2.410	2.410	2.302	2.307	2.416	2.396
Mulliken net charges								
Cu1	+0.0179	−0.0849	+0.0245	−0.0974	−0.1071	−0.0839	−0.1114	−0.0794
Cu2	+0.1059	+0.0144	+0.0910	−0.0224	+0.0207	−0.0535	−0.0195	−0.0505
Cu_3	–	–	+0.0747	−0.1373	+0.1323	+0.1670	+0.1288	+0.1636
Cu_4	–	–	–	–	+0.0656	−0.1115	−0.0570	−0.0960
Cu_5	–	–	–	–	–	–	+0.1204	+0.1627

RESULTS AND DISCUSSION

Previous calculations by Ahlrichs and coworkers [4, 7, 8] have shown that the Cu_{12} core of the hypothetical bare cluster $Cu_{12}Se_6$ is a regular cuboctahedron. This cuboctahedral core is distorted upon linking of phosphine ligands into two types of structural isomers observed for $Cu_{12}E_6(PR_3)_8$ (E = S, Se) species [3]. These isomers differ by the respective position on the cuboctahedron of the 8 copper atoms which are bonded to a phosphine ligand. It has been shown that the energy difference between them is small [7]. In this paper we discuss only the isomer architecture of which is related to the SA, i.e., in which the phosphine ligands are coordinating copper atoms making two opposite squares of the Cu_{12} cuboctahedron. In this case, Ahlrichs and coworkers have shown that the addition of 8 phosphine ligands to $Cu_{12}Se_6$ induces a distortion of the Cu_{12} from O_h (cuboctahedron) to D_{4h} (two fused Cu_8 square antiprisms) [4], a structure in agreement with the X-ray structure of $Cu_{12}Se_6(PEtPh_2)_8$ [4] and related species [3]. The distortion of the metallic core upon addition of the eight phosphine ligands is sketched at the top of Fig. 3. It provides 8 additional Cu…Cu contacts. Our DFT geometry optimizations on **1** found the same distortion upon phosphine addition. As usually found for this type of calculations containing electron-rich metal clusters [2c], the bond distances are systematically overestimated by ~4–6%. Apart from this cluster special expansion when going from the experimental compound $Cu_{12}Se_6(PEtPh_2)_8$ [4] to the DFT optimized model 1, there is a good agreement between both geometries, which are consistent with the presence of some Cu…Cu bonding.

To understand the O_h to D_{4h} distortion upon phosphine addition, one has to consider first that the cuboctahedral $Cu_{12}Se_6$ naked cluster is made of 12 interacting $CuSe_{2/4}$ units. The frontier orbital (FO) pattern of such bent ML_2-type fragments is well-known [13]. It is sketched on the left side of Fig. 4. It is made of two vacant 4s/4p orbitals (one of σ-type and one of π-type) lying far above a block of five low-lying occupied 3d levels. In the cuboctahedral $Cu_{12}Se_6$ cluster the 12 $CuSe_{2/4}$ centers interact in the way depicted in the middle of Fig. 4. The contracted Cu 3d AOs overlap rather weakly to give rise to a set of 60 occupied combinations which are nonbonding, weakly bonding or weakly antibonding. Overall, the 3d interactions are somewhat destabilizing since all of these combinations are occupied. The more diffuse 4s/4p FOs overlaps significantly. From group theory considerations one can predict that their combinations separate into two groups (a bonding one and an antibonding one) of 12 vacant orbitals. Significant overlap between the 4s/4p FOs leads to a significant energy separation between these two groups of combinations. The

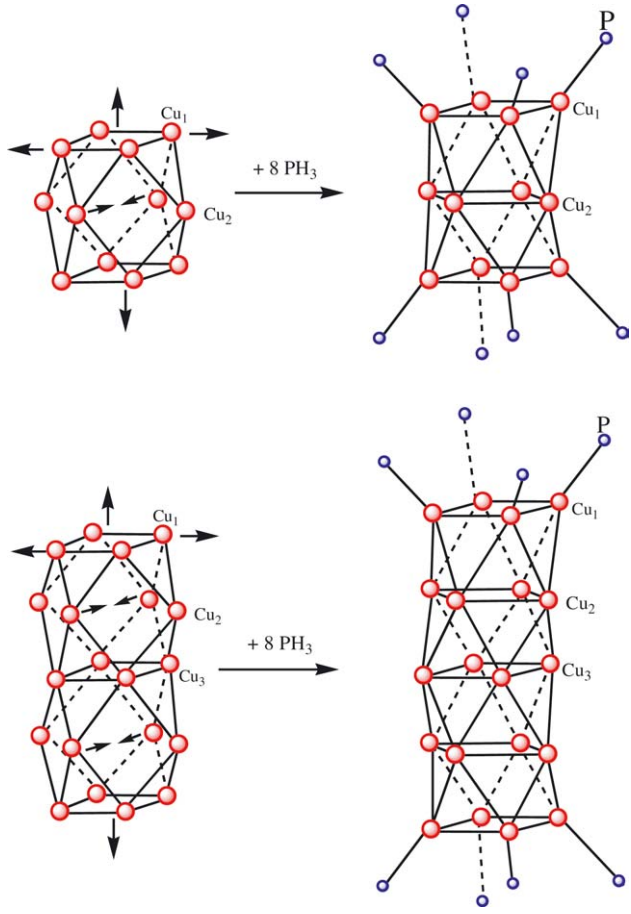

Fig. 3. The cuboctahedral–square antiprismatic distortion of $Cu_{12}Se_6$ (top) and $Cu_{20}Se_{10}$ (bottom) upon addition of eight phosphine ligands.

12 bonding combinations correspond to the following irreducible representations: t_{2g}, t_{1u}, t_{2u}, e_g and a_{2u}. Being the lowest unoccupied FOs, these 12 bonding combinations constitute the set of potential accepting orbitals of $Cu_{12}Se_6$.

When the cuboctahedral (O_h) to fused square antiprismatic (D_{4h}) distortion is applied to the $Cu_{12}Se_6$ naked cluster, 8 of the 12 4s/4p bonding combinations are stabilized, due to their significant $Cu_p \ldots Cu_p$ bonding character, as sketched on the right side of Fig. 4. In the D_{4h} symmetry, they span a_{1g}, a_{2u}, b_{1g}, b_{2u}, e_g and e_u symmetry. They have exactly the

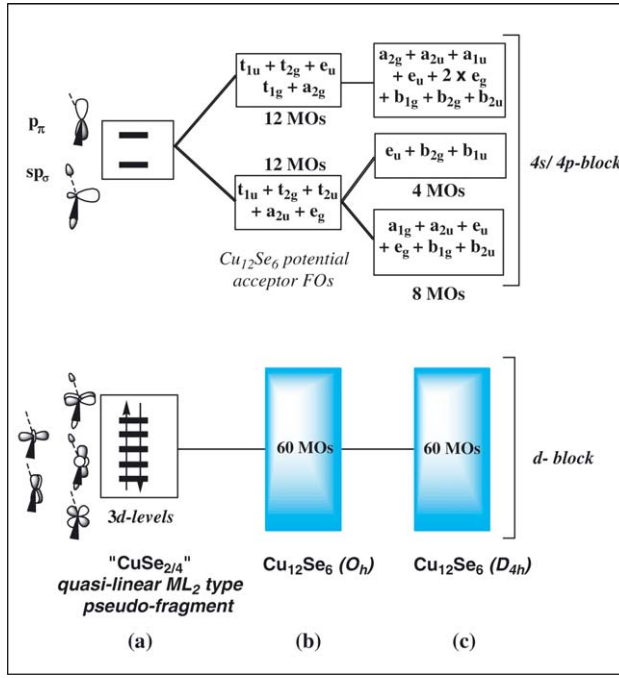

Fig. 4. (a) $CuSe_{2/4}$ FMOs; (b) $Cu_{12}Se_6$ FMOs in the cuboctahedral O_h symmetry; (c) $Cu_{12}Se_6$ FMOs in the fused antiprismatic D_{4h} symmetry.

same symmetry as the 8 combinations of the 8 orbitals associated with the phosphine lone pairs of $Cu_{12}Se_6(PR_3)_8$. Thus, the O_h to D_{4h} distortion allows better metal–phosphine bonding. The computed occupations of these eight accepting frontier orbitals of the $Cu_{12}Se_6$ fragment in **1** is 0.40, 0.23, 0.40, 0.34, 2×0.36 and 2×0.36, respectively.

As mentioned previously, the Cu_{20} core of $Cu_{20}Se_{10}(PPh_3)_8$ [4] can be described as resulting from the fusion of four face-sharing antiprisms. We have optimized the geometries of the $Cu_{20}Se_{10}$ naked cluster and of model **2**. As one can see from the optimized Cu…Cu bond distances (Table I), the naked cluster is better described as made of 2 fused cuboctahedra. Thus, the addition of 8 phosphines to this cluster induces the same type of cuboctahedral to square antiprismatic distortion as for the $Cu_{12}Se_6$ cluster. The orbital explanation for this distortion is similar to that provided above for the Cu_{12} series, i.e., it causes the stabilization of the 8 FOs of the $Cu_{20}Se_{10}$ fragment which will participate to the 8 Cu-P bonds, thus strengthening these bonds. This is exemplified by the occupation of

these frontier orbitals in the final compound which are 0.35, 0.36, 0.42, 0.42, 2×0.50 and 2×0.32 for the a_{1g}, a_{2u}, b_{1g}, b_{2u}, e_g and e_u symmetries, respectively.

In some large nuclearity metal clusters, the most bonding combination of the vacant σ-type metal hybrids can be so low in energy that it reaches the d-band and therefore requires to be occupied by the closed-shell requirement principle [14]. We have checked this possibility by calculating the largest hypothetical clusters of this type that we could afford at a reasonable computer time cost, namely $Cu_{28}Se_{14}(PH_3)_8$ (**3**) and $Cu_{36}Se_{18}(PH_3)_8$ (**4**), the metallic core of which results from the fusion of 6 and 8 square antiprisms, respectively (Fig. 1). The computed HOMO-LUMO gaps of **3** and **4** are small (Fig. 2) since 2 bonding combinations of vacant 4s/4p Cu orbitals, of a_{1g} and a_{2u} symmetry, are rather low lying in energy. This suggests the possibility for stable $\mathbf{3}^{2-}$ and $\mathbf{4}^{2-}$ dianions which would formally contain two Cu^0 atoms. Calculations on these dianions yielded HOMO-LUMO gaps larger than their neutral relatives (Fig. 2) and a significant shortening of some Cu…Cu distances (Table I). Such a shortening upon populating the LUMO of **3** or **4** should also occur in their excited triplet state of their neutral form, suggesting the possible luminescence properties associated with a significant Stokes shift caused by the variation of the Cu…Cu distances between the singlet ground state and the excited triplet state.

Finally, it is interesting to mention that all the computed Cu…Cu Mulliken overlap populations indicate weak but significant bonding (Table I). The strongest interaction corresponds to the intrasquare $Cu_1 \ldots Cu_2$ contacts in all the computed models, which is, consistently, one of the shortest optimized Cu…Cu distance.

CONCLUSION

Calculations on the $Cu_{2(4n+2)}Se_{4n+2}(PH_3)_8$ ($n = 1, 2, 3, 4$) series of D_{4h} symmetry indicate that the fused square antiprismatic structure of the metal framework is preferred over the fused cuboctahedral one because it reinforces the Cu–P bonds. Thus, the presence of the terminal phosphine ligands tends to strengthen the mixing of bonding combinations of the vacant Cu 4s and 4p orbitals into the occupied 3d combinations. This through-bond effect is of course stronger in the close vicinity of the phosphines. Nevertheless, for all the compounds the strongest Cu…Cu bonding interaction is the intrasquare Cu_1–Cu_2 one. It is interesting to mention that the distortion of the cuboctahedron to the fused SA structure is associated with local Se–Cu–Se bending which is required for tricoordination, as discussed recently by Carvajal *et. al.* [15]. As expected, the computed

HOMO-LUMO gap decreases with the cluster size and the largest clusters are easy to reduce by populating a low-lying LUMO which is of Cu…Cu bonding character, leading to stable dianionic species. Extrapolation of the HOMO-LUMO gap variation leads to predict a limit value of ~0.17 eV for the infinite one-dimensional Cu_2Se species.

ACKNOWLEDGMENTS

We thank the Agence Universitaire de la Francophonie for a 9-month research stay grant of B. Z. in Rennes. This work was also supported by the Algerian-French program 02MDU552. Computing facilities were provided by the PCIO of Rennes and the IDRIS-CNRS of Orsay.

REFERENCES

1. (a) D. Fenske, J. Ohmer, J. Hachgenei, and K. Merzweiler (1988). *Angew. Int. Ed. Engl.* **27**, 1277. (b) D. Fenske. *in Clusters and Colloids: From Theory to Applications,* G. Schmid (ed.), (Wiley-VCH, Weinheim, 1994), p. 212. (c) G. Henkel and S. Weissgraeber *in Metal Clusters in Chemistry*, P. Braunstein, L. Oro, and P. R. Raithby (Ed.), (Willey-VCH, Weinheim, 1999), Vol. 3, p. 163.
2. (a) J.-F. Halet and J.-Y. Saillard (1997). *Struct. Bonding* **87**, 81. (b) R. Gautier, J.-F. Halet, J.-Y. Saillard, *In Metal Clusters in Chemistry*. P. Braunstein, L Oro, P. R Raithby (eds.), (Wiley-VCH, Weinheim, 1999), Vol. 3, p. 1643. (c) M. T. Garland, J.-F. Halet, and J.-Y. Saillard (2001). *Inorg. Chem.* **40**, 3342.
3. S. Dehen, A. Eichhöfer, and D. Fenske (2002). *Eur. J. Inorg. Chem.* 279.
4. (a) S. Dehnen, A. Schäfer, D. Fenske, and R. Ahlrichs (1994). *Angew. Chem. Int. Ed. Engl.* **106**, 746.
5. (a) P. K. Mehrota and R. Hoffmann (1978). *Inorg. Chem.* **17**, 2187. (b) D. F. Shriver, H. D. Kaesz, and R.D. Adams (1990). *The Chemistry of Metal Cluster Complexes* (VCH, New. York).
6. P. Pyykkö (1997). *Chem. Rev.* **97**, 597.
7. A. Schäfer and R. Ahlrichs (1994). *J. Am. Chem. Soc.* **116**, 10686.
8. K. Eichkorn, S. Dehnen, and R. Ahlrichs (1998). *Chem. Phys. Lett.* **284**, 287.
9. *ADF2.3* and *ADF2002.01*; SCM: Theoretical Chemistry, Vrije Universiteit, Amsterdam, The Netherlands, http://www.scm.com. (a) E. J. Baerends, D.E. Ellis, and P. Ros (1973). *Chem. Phys.* **2**, 41. (b) E. J. Baerends, D.E. Ellis, and P. Ros (1978). *Int. J. Quantum. Chem.* **S12**, 169. (c) P. H. Boerrigter, G. te Velde, and E. J. Baerends (1988). *Int. J. Quantum. Chem.* **33**, 87. (d) G. te Velde and E. J. Baerends (1992). *J. Comput. Phys.* **99**, 84. (e) C. Fonseca Guerra, J. G. Snijders, G. te Velde, and E. J. Baerends (1998). *Theor. Chem. Acc.* **99**, 391. (f) G. te Velde, F. M. Bickelhaupt, S. J. A. van Gisbergen, C. Fonseca Guerra, E. J. Baerends, J. G. Snijders, and T. Ziegler (2001). *J. Comput. Chem.* **22**, 931.
10. S. Vosko, L. Wilk, and M. Nusair (1990). *Can. J. Chem.* **58**, 1200.
11. (a) A. D. Becke (1986). *J. Chem. Phys.* **84**, 4524. (b) A. D. Becke (1988). *Phys. Rev. A* **84**, 4524.
12. (a) J. P. Perdew (1986). *Phys. Rev. B* **33**, 8882. (b) J. P. Perdew (1986). *Phys. Rev. B* **34**, 7406.

13. T. A. Albright, J. K. Burdett, and M.-H. Whangbo (1985) *Orbital Interactions in Chemistry* (Wiley, New York).
14. (a) R. Gautier, E. Furet, J.-F. Halet, Z. Lin, J.-Y. Saillard, and Z. Xu (2002). *Inorg. Chem.* **41**, 796.
15. M. A. Carvajal, J. J. Novoa, and S. Alvarez (2004). *J. Am. Chem. Soc.* **126**, 1465.